Spectrochimica Acta Part A: Molecular and Biomolecular Spectroscopy 134 (2015) 484–492

Contents lists available at ScienceDirect

Spectrochimica Acta Part A: Molecular and Biomolecular Spectroscopy

journal homepage: www.elsevier.com/locate/saa

Copper(II) complexes with 4-hydroxyacetophenone-derived acylhydrazones: Synthesis, characterization, DNA binding and cleavage properties

Ramazan Gup [a,*], Cansu Gökçe [a], Selçuk Aktürk [b]

[a] Department of Chemistry, Mugla Sıtkı Koçman University, 48100 Mugla, Turkey
[b] Department of Physic, Mugla Sıtkı Koçman University, 48100 Mugla, Turkey

HIGHLIGHTS

- Two new Cu(II) complexes of Schiff base-hydrazone ligands have been synthesized and characterized.
- The interaction of the copper(II) complexes exhibit different non-covalent binding behavior.
- The complexes efficiently cleavage pBR322 DNA through oxidative mechanism.

GRAPHICAL ABSTRACT

New Schiff base-hydrazone ligands have led to two new copper complexes binding to the DNA through non-covalent mode and act as good metallonucleases through oxidative cleavage mechanism. The effect of complex concentration on the DNA cleavage reactions has also investigated. X-ray powder diffraction illustrates that $[Cu(L^2)_2]$ complex is crystalline in nature while $[Cu(H_2L^1)_2]$ has an amorphous structure.

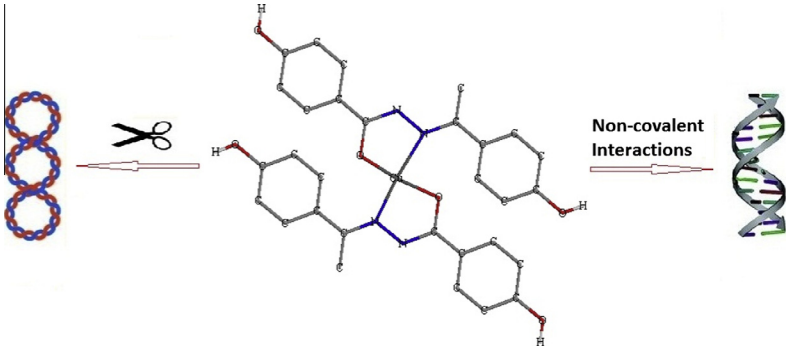

ARTICLE INFO

Article history:
Received 28 March 2014
Received in revised form 22 May 2014
Accepted 25 June 2014
Available online 3 July 2014

Keywords:
Acylhydrazone
Copper(II) complex
DNA binding
DNA cleavage

ABSTRACT

Two new Cu(II) complexes of Schiff base-hydrazone ligands, hydroxy-N′-[(1Z)-1-(4-hydroxyphenyl)ethylidene]benzohydrazide $[H_3L^1]$ and ethyl 2-(4-(1-(2-(4-(2-ethoxy-2-oxoethoxy)benzoyl)hydrazono)ethyl)phenoxy)acetate (HL^2) have been synthesized and then characterized by microcopy and spectral studies. X-ray powder diffraction illustrates that $[Cu(L^2)_2]$ complex is crystalline in nature whereas $[Cu(H_2L^1)_2]\cdot 2H_2O$ has an amorphous structure. Binding of the copper complexes with Calf thymus DNA (CT-DNA) has been investigated by UV-visible spectra, exhibiting non-covalent binding to CT-DNA. DNA cleavage experiments have been also investigated by agarose gel electrophoresis in the presence and absence of an oxidative agent (H_2O_2). The effect of complex concentration on the DNA cleavage reaction has been also studied. Both copper complexes show nuclease activity, which significantly depends on concentrations of the complexes, in the presence of H_2O_2 through oxidative mechanism whereas they slightly cleavage DNA in the absence an oxidative agent.

* Corresponding author. Tel.: +90 252 2111496; fax: +90 252 2111472.
E-mail address: rgup@mu.edu.tr (R. Gup).

http://dx.doi.org/10.1016/j.saa.2014.06.133
1386-1425/

Introduction

Schiff base-hydrazones and their metal complexes have received much attention in the fields of chemistry and biology due to their broad spectrum of activities. They have a variety of applications in biological and clinical fields. They denote *anti*-bacterial, *anti*-fungal, *anti*-convulsant, *anti*-inflammatory, *anti*-malarial, analgesic, *anti*-platelets, *anti*-tuberculosis, *anti*-cancer and insecticidal activities [1–8]. The significant biological activity of the acylhydrazones and the dependence of their mode of chelation with transition metal ions present in the living systems have been of significant interest [9–12]. Transition metal complexes of acylhydrazones are also known to provide useful models for elucidation of the mechanisms of enzyme inhibition [13,14]. They act as good potential oral drugs to treat the genetic disorders such as thalassemia [15].

DNA-transition metal complex interaction has been of interest because of its possible application in molecular biology [14,15] and cancer therapy [16–18]. Coordination compounds show unique chemical and physical properties as well as the abilities of their ligands to be adjusted to DNA interaction activities. Copper is an important trace element for life and is involved in complex formation in a number of biological processes. Copper(II) complexes have been used as for the treatment of many diseases including cancer [19,20]. Therefore, investigations on copper complexes are becoming more prominent in the research area of bioinorganic chemistry [21–28]. Herein, we described the synthesis and characterization of new Cu(II) complexes of hydrazone Schiff base ligands and their DNA binding and cleavage activities.

Experimental section

Material and methods

All chemicals used were analytical reagent grade. Copper(II) acetate, ethyl 4-hydroxybenzoate, 4-hydroxyacetophenonee, ethyl bromoacetate, K_2CO_3, acetone and hydrazine monohydrate were purchased from Fluka and Sigma-Aldrich and used without further purification. Calf thymus DNA (CT-DNA) was purchased from Sigma-Aldrich. pBR322 DNA was purchased from Fermantas. ^1H and ^{13}C NMR spectra were recorded on a Bruker 400 MHz spectrometer in DMSO_d_6 with TMS as the internal standard. IR spectra were recorded on pure solid samples with a Thermo-Scientific, Nicolet iS10-ATR. The electronic spectra of the ligands and complexes were recorded on a PG Instruments T80+ UV/Vis Spectrophotometer. Carbon, hydrogen and nitrogen analyses were carried out on a LECO 932 CHNS analyzer and copper content was determined by atomic absorption spectroscopy using the DV 2000 Perkin Elber ICP-AES. Mass spectra were recorded on a Waters Xevo TQ-S UPLC-MS/MS spectrometer. Room temperature magnetic susceptibility measurements were carried out on powdered samples using a Sherwood Scientific MK1 Model Gouy Magnetic Susceptibility Balance. The thermogravimetric analysis was carried out in dynamic nitrogen atmosphere (20 mL min^{-1}) with a heating rate of 20 °C min^{-1} using a Perkin Elmer Pyris 1 TGA thermal analyzer in the Central Laboratory at METU. Powder X-ray diffraction (XRD) patterns were collected using Cu Kα monochromatic radiation (λ = 1.54056 Å) at room temperature on a Rigaku-SmartLab diffractometer. Scanning electron microscopy (SEM) was performed using a JEOL SEM 7700F. Local composition was analyzed by energy-dispersive X-ray spectroscopy (EDS) with an analyzer system attached to a JEOL SEM 7700F. High-resolution transmission electron microscopy (HRTEM) was performed using a JEOL JEM 2100F electron microscope. XRD, SEM-EDS and HRTEM investigations were performed in the Research Centre Laboratory at Mugla Sıtkı Koçman University.

Synthesis of H_3L^1

This compound was prepared by small changing the method of Rajput and Rajput [21] as follows: 4-hydroxyacetophenone (1 mmol, 0.136 g) dissolved in ethanol (10 mL) was added drop wise to a suspension of 4-hydroxybenzohydrazide (II) (1 mmol, 0.152 g) with a catalytic amount of glacial acetic acid in ethanol (10 mL) in room temperature. The reaction mixture was refluxed for further 4 h. On standing over night, the white crystalline product separated, collected by filtration, washed with small amount of diethyl ether and then dried in vacuum. Yield 81%; Mp 285–287 °C (Lit 274–276 °C); UV (DMF, nm) 267, 304; IR (ATR, cm^{-1}) 3285 (OH), 1625 $(C{=}O)_{amide}$, 1617 (C=N), 1369 (C—N), 1257 and 1172 (C—O—C); ^1H NMR (DMSO_d_6, ppm) δ 2.27 (s, 3H, N=C—CH_3), 6.78 (d, 2H, J = 8.5, ArH), 6.82 (d, 2H, J = 8.6, ArH), 7.67, (d, 2H, J = 8.5, ArH), 7.77, (d, 2H, J = 8.6, ArH), 9.93 (s, 2H, OH), 10.41 (s, 1H, NH); ^{13}C NMR (DMSO_d_6, ppm) 161.1 (C=O), 160.7 (C=N), 159.3 (*C*—O), 130.5, 129.7, 129.5, 128.6, 125.3, 115.8, 115.5 (Ar—C)), 19.8 (CH_3). Analysis (%Calculated/found) for $C_{15}H_{14}N_2O_3$ C: 66.66/66.78, H: 5.22/5.10, N: 10.36/10.69.

Synthesis of HL^2

A mixture of H_3L^1 (1 mmol, 0.270 g), ethyl bromoacetate (2 mmol, 0.334 g) and dry K_2CO_3 (10 mmol, 0.276 g) in 25 mL acetone was refluxed with stirring for 40 h and poured to 200 mL of cold water. The white precipitate formed was filtered and washed with water and finally recrystallized from acetone-water. Yield 40%; Mp 115 °C; UV (EtOH, nm) 250, 300, IR (ATR, cm^{-1}) 3365 (NH), 2911–2979 $(CH)_{aliphatic}$ 1755 $(C{=}O)_{ester}$, 1657 $(C{=}O)_{amide}$, 1605 (C=N), 1385 (C—N), 1255 and 1082 (C—O—C); ^1H NMR (DMSO_d_6, ppm) δ 1.18–1.23 (tt, 6H, J = 7.0, CH_3), 2.30 (s, 3H, N=C—CH_3), 4.13–4.20 (q, J = 7.0, 4H, OCH_2CH$_3$), 4.82 (s, 2H, Ar—OCH_2) and 4.87 (s, 2H, Ar—OCH_2), 6.95 (d, 2H, J = 8.8, ArH), 7.01 (d, 2H, J = 8.8, ArH), 7.77 (d, 2H, J = 4.7, ArH),7.85 (d, 2H, J = 8.2, ArH), 10.58 (s, 1H, NH); ^{13}C NMR (DMSO_d_6, ppm) 169.3 and 169.2 $(C{=}O)_{ester}$, 161.8 $(C{=}O)_{amide}$, 159.3 (C=N), 131.9, 130.4, 128.5, 127.6, 115.0, 114.8 (Ar—C), 65.3 and 65.2 (O$\underline{C}H_2$), 61.5 and 61.4 (COO$\underline{C}H_2$), 21.1 ($\underline{C}H_3$—C=N), 14.8 and 14.7 ($\underline{C}$H3). Analysis (%Calculated/found) for $C_{23}H_{26}N_2O_7$ C: 62.43/62.16, H: 5.92/5.88, N: 6.33/6.57.

Synthesis of Cu(II) complexes

A solution of 1 mmol copper(II) acetate dihydrate (0.20 g) in EtOH (10 mL) was added to a hot solution containing 2 mmol H_3L^1 (0.54 g) or HL^2 (0.884 g) in absolute ethanol (15 mL) with stirring. The reaction mixture was refluxed for 3 h and then the solvent was evaporated under reduced pressure. The precipitated complexes were filtered off and finally washed with small amount of cold water.

For $[Cu(H_2L^1)_2]\cdot 2H_2O$: Dark green complex; yield: 85%; m.p.: 219 °C. μ_{eff} = 1.71 B.M.; UV (DMF, nm) 276, 308, 363 sh, 380, 403 sh; FT-IR (ATR, cm^{-1}) 3182 b (O—H), 1604 m (C=N—N=C), 1362 (C—N), 1253 s and 1165 m (C—O—C). MS (ES^+), (m/z): 602.76 $[M]^+$. Analysis (%Calculated/found) for $C_{30}H_{30}CuN_4O_8$ C: 56.47/56.24, H: 4.74/4.57, N: 8.78/8.52, Cu: 9.96/10.22.

For $[Cu(L^2)_2]$: Light brown complex; yield: 79%; m.p.: 187 °C. μ_{eff} = 1.73 B.M.; UV (DMF, nm) 269, 306 and 354; FT-IR (ATR, cm^{-1}) 3449 (O—H), 1752 $(C{=}O)_{ester}$, 1604 (C=N—N=C), 1248 and 1165 (C—O—C). MS (ES^+), (m/z): 947.50 $[M]^+$. Analysis (%Calculated/found) for $C_{46}H_{44}CuN_4O_{14}$ C: 58.37/58.42, H: 5.32/5.26, N: 5.92/5.85, Cu: 6.91/6.85.

DNA binding

Electronic absorption titrations

All the experiments involving the interaction of the complexes with CT-DNA were carried out in water buffer containing 5 mM tris [tris(hydroxymethyl)aminomethane] and 50 mM NaCl, and adjusted to pH 7.3 with HCl. The solution of CT-DNA in the buffer gave a ratio of UV absorbance of 1.8–1.9:1 at 260 and 280 nm, indicating that the CT-DNA was sufficiently free of protein [22]. The CT-DNA concentration per nucleotide was determined spectrophotometrically by employing an extinction coefficient of 6600 M^{-1} cm^{-1} at 260 nm [23]. An appropriate amount of the copper complexes was dissolved in a solvent mixture of 1% DMF and 99% tris–HCl buffer. Absorption titration experiments were performed by maintaining the metal complex concentration as constant while gradually increasing the concentration of the CT-DNA within 0–100 μM.

Chemical nuclease activity

pBR322 plasmid DNA was used for all cleavage activities. In a typical experiment, 7 μl plasmid DNA (50 ng/μl) was mixed with different concentrations of complexes (10, 25, 50, 75 and 100 μM dissolved in DMF) to determine optimum activation concentration. 5 μl H_2O_2 (5 mM) was added to mixture to oxidize the reactant. Finally the reaction mixture was diluted with the Tris buffer (100 mM Tris, pH: 8) to a total volume of 30 μl. After that reaction mixtures were incubated at 37 °C for 2 h. Samples (20 μl) were then loaded with 4 μl loading dye (0.25% bromophenol blue, 0.25% xylene cyanol,30% glycerol, 10 mmol EDTA) on a%1 agarose gel containing 1 μg/ml of EtBr. The gel was run at 100 V for 3 h in TBE buffer and photographed under UV light. To test for the presence of reactive oxygen species generated during strand scission, reactive oxygen intermediate scavengers, that is, SOD, DMSO, KI and NaN_3 were added alternately to the reaction mixture. Samples were treated as described above.

Results and discussion

Synthesis and characterization

The bidentate hydrazone Schiff base (H_3L^1) was easily prepared according to the previously reported method with small change [21]. The reaction of this compound with ethyl bromoacetate in the presence of dry K_2CO_3 in dry acetone gave the other Schiff base–hydrazone ligand (HL^2) bearing ester group which was reported for the first time in this work (Scheme 1). The copper(II) complexes were synthesized by the reaction of the synthesized acylhydrazone with copper(II) acetate in ligand to copper ratio of 2:1. The nature of bonding and geometry of the Cu(II) complexes as well as Schiff base hydrazones were deduced from elemental analysis, various spectroscopies (IR, UV–Vis, ^{1}H NMR, ^{13}C NMR, mass) and microscopies (TEM, SEM-EDS), magnetic susceptibility measurements, thermal gravimetric analysis (TGA), and powder X-ray diffraction (XRD) techniques.

^{1}H and ^{13}C NMR spectroscopy

The main ^{1}H NMR signals for each of the acylhydrazone compounds in DMSO_d_6 are given in the experimental section. Formation of the HL^2 is confirmed by the absence of the OH proton signal at 9.93 ppm assigned to the starting material H_3L^1. The D_2O exchangeable resonances appeared at 10.41 and 10.58 ppm for H_3L^1 and HL^2 ligands are assigned to NH protons [24–28]. The NMR spectra of HL^2 shows two signals for each hydrogen of the carboxylic ester parts possibly due to unsymmetrical nature of two ester groups of HL^2. For instance, two different chemical shift values for the methylene protons of —$\underline{CH_2}$OPh have been observed as a singlet at 4.82 and 4.87 ppm, suggesting these methylene protons at the each ester groups is not equal. Accordingly, two quartets and triplets almost overlapping with one another are observed for the other methylene (O$\underline{CH_2}$) and methyl (—$CH_2\underline{CH_3}$) protons of the carboxylic ester groups (Fig. S1).

The ^{1}H NMR spectral assignments of the new acylhydrazone compounds are also supported by the ^{13}C NMR spectrum. The characteristic chemical shifts of the amide carbonyl (C9) and azomethine (C10) groups of the acylhydrazones are observed at 161.1 and 160.7 ppm and 161.8 and 159.3 ppm for H_3L^1 and HL^2 ligands, respectively. In the ^{13}C NMR spectra of the HL^2 the signals at 169.3 and 169.2 ppm are assignable to the carbonyl carbons of ester groups (C3 and C15). Similarly to the ^{1}H NMR spectra, two signals are observed for the each carbon of the two ester parts of the HL^2 (C4 and C14, C2 and C16, C1 and C17) probably due to unsymmetrical nature of these groups. The chemical shifts for the carbon atoms of the aromatic rings are recorded between 114.8 and 159.3 ppm. These assignments are in good agreement with those previously reported for similar compounds [29–34]. These results strongly suggest that the proposed acylhydrazone compound has been formed. Furthermore, in the ^{1}H and ^{13}C NMR spectra of the H_3L^1 and HL^2 only one signal has observed for each hydrogen and carbon indicating that both acylhydrazones are the E configuration (Fig. 1) [24,25,29–31].

IR spectroscopy

In the IR spectra of the H_3L^1, the vibration band of ν(O—H) is observed at 3285 cm^{-1} which disappears in the IR spectrum of HL^2 indicating that condensation takes place. The stretching vibrations of amide I and imine groups are observed at 1625 and 1617 cm^{-1}, 1657 and 1605 cm^{-1} for H_3L^1 and HL^2, respectively. On the other hand, the band observed at 1755 cm^{-1} is assigned to the stretching vibration of the ester carbonyl which is also characteristic for carboxylic esters (Fig. S2). The amide NH stretching band of H_3L^1 is not observed in the IR spectra probably due to overlapping with the broad OH stretching frequency. However, this band is observed clearly at 3365 cm^{-1} in IR spectra of the HL^2 ligand which is hydroxyl group free [24–27,30,31].

In the IR spectra of the copper(II) complexes, the amide I and *ν*(N-H) stretching bands disappear and a new band appears at 1604 cm-1 probably due to >C═N—N═C< stretching vibration indicating transformation of the carbonyl group to its enolic form through keto-enol tautomerism and subsequent coordination of the enolic oxygen to metal after deprotonation [27–32]. Therefore, from the IR spectra it is concluded that the acylhydrazones act as mono anionic bidentate ligands coordinating through the azomethine nitrogen and the enolic oxygen (Fig. 2). In addition, the bands due to the carbonyl of the carboxylic ester and phenolic OH vibrations remain unaltered, suggesting non-involvement of these groups in the complex formation (Fig. S3). In the mass spectra of the complexes, the presence of molecular ion peaks at m/z = 602.76 $[M]^+$ for $[Cu(H_2L^1)_2]$ and 947.45 $[M]^+$ for $[Cu(L^2)_2]$ confirm the proposed structures.

Electronic absorption spectra

The ligands exhibit a band around 267 nm and 250 nm for H_3L^1 and HL^2, respectively, assignable to the aromatic ring transition $\pi \rightarrow \pi^*$. The intense bands observed at 304 nm for H_3L^1 and 300 nm for HL^2 can be assigned the n→π∗ type electronic transitions. In the copper(II) complexes, these bands undergo slight bathochromic shift to 308 and 306 nm for $[Cu(H_2L^1)_2]$ and $[Cu(L^2)^2]$, respectively, and the intensities of these bands are also

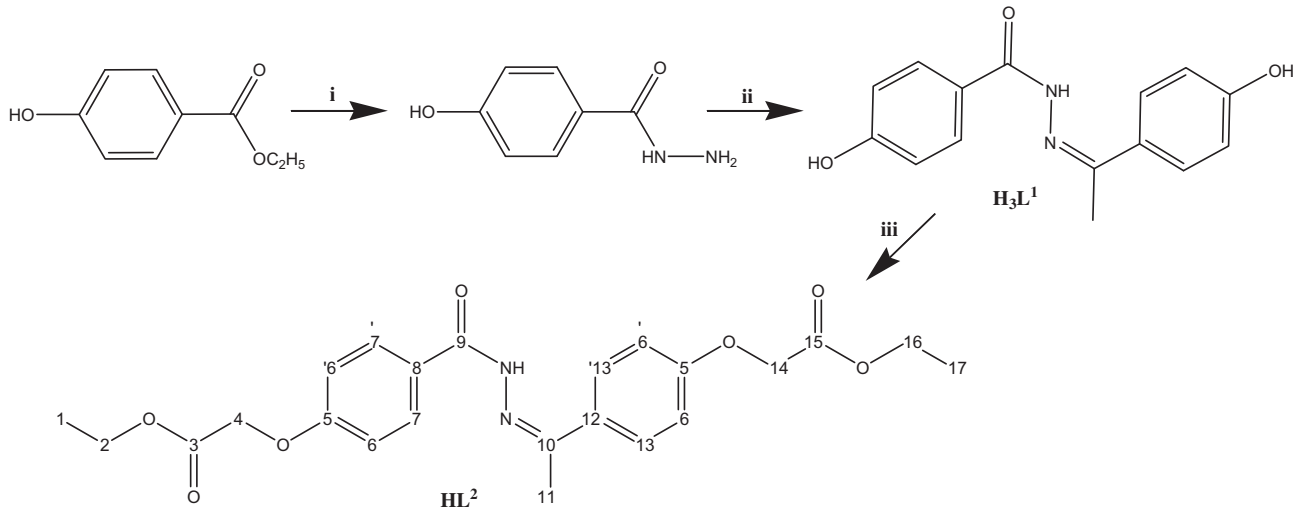

Scheme 1. Schematic diagram showing the synthesis of the acylhydrazone ligands. **i**, $NH_2NH_2{\cdot}H_2O$, EtOH, reflux 4 h. **ii,** 4-hydroxyacetophenone, EtOH, AcOH, reflux 5 h; **iii,** ethyl bromoacetate, K_2CO_3, acetone, reflux 40 h.

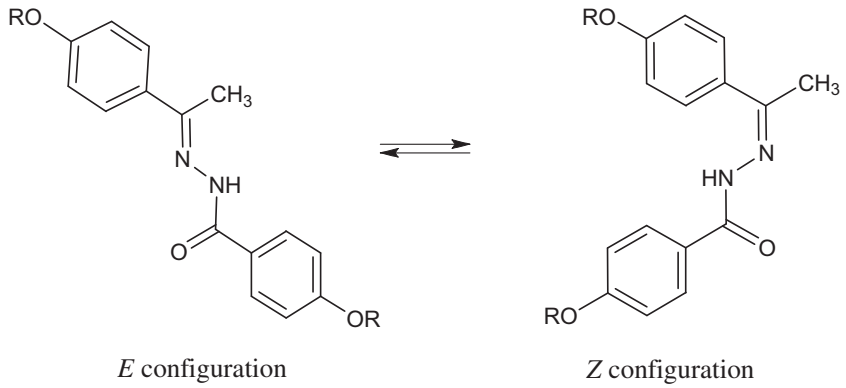

Fig. 1. Structural configurations of the Schiff base-hydrazones.

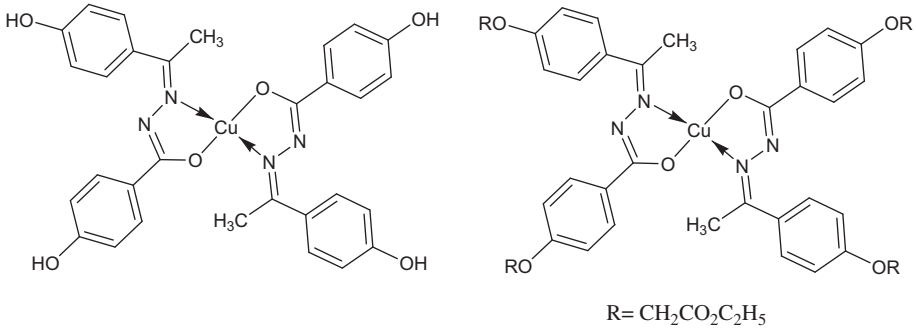

Fig. 2. Suggested structures of the copper(II) complexes.

increased. The electronic spectrums of copper complexes show the metal-to-ligand charge transfer bands at 380 nm and 354 nm for $[Cu(H_2L^1)_2]$ and $[Cu(L^2)_2]$ complexes, respectively, which is comparable to those of previously reported complexes [24–28]. In the visible region, there is a shoulder at 403 nm for $[Cu(H_2L^1)_2]$ which is also probably due to allowed charge-transfer transition. Unfortunately the expected weak d–d transition in the visible region for the paramagnetic copper complexes cannot be detected even with concentrated solutions. It may be lost in the low energy tail of the charge transfer transition [24–27]. The observed magnetic moment values for $[Cu(H_2L^1)_2]$ and $[Cu(L^2)_2]$ complexes are 1.71 and 1.73 BM, respectively, which are consistent with the expected spin-only magnetic moment of an S = 1/2 (1.73 BM), Cu(II) d^9 system.

X-ray diffraction analysis

Single crystal XRD could not be employed to confirm the structures of the complexes since attempts to isolate crystals suitable for single X-ray diffraction were unsuccessful. To obtain further evidence about the structure of the copper complexes, powder XRD pattern of the complexes were recorded over at 2θ = 10–70°

range and XRD patterns are shown in Figs. S4 and S5. One of the copper complexes, $[Cu(L^2)_2]$, displays sharp crystalline peaks indicating their crystalline nature, whereas the other complex, $[Cu(H_2L^1)_2]\cdot 2H_2O$, does not exhibit well-defined crystalline peak possibly due to its amorphous nature. The average crystallite sizes of the $[Cu(L^2)_2]$ were complex calculated using Scherre's formula. The complex has an average crystallite size of 52 nm, suggesting that it is in nanocrystalline phase.

SEM and EDS analyses

The surface morphologies of Schiff base-hydrazones and their copper(II) complexes were observed by scanning electron microscope (SEM). The SEM micrographs were taken at 15 kV accelerating voltage and magnification was fixed according to ×500 shown in Figs. 3 and 4. The SEM micrograph of H_3L^1 ligand in Fig. 3a shows a polycrystalline morphology with agglomerated nano rods, and the presence of particles are randomly distributed. On the other hand, from the SEM micrograph of the copper complex of this ligand, $[Cu(H_2L^1)_2]$ (Fig. 3b), it is clearly seen that the surfaces of these particles with different sizes appear to be smooth and porous. The average particle sizes for H_3L^1 and its Cu(II) complex are ~10 μm and ~100 μm respectively. The SEM micrograph of HL^2 (Fig. 4a) exhibits a square single phase having layer by layer with irregular boundary in different micrometer size whereas its copper complex, $[Cu(L^2)_2]$, has a homogeneous phase with non-uniform needles. The average sizes of these particles are nearly 50 μm. From SEM micrograph, it is clear that there is a strong change in morphology of the acylhydrazone ligands after coordination to copper ion.

Energy dispersive spectroscopy (EDS) allows determining the chemical composition of a sample. Therefore, the compositions of both ligands and copper complexes were defined by EDS analysis shown in Figs. 5 and 6. By comprising the EDS spectrum of the ligands and copper complexes it is concluded that each aroylhydrazone ligands contains only C, N, O atoms whereas their complexes have just C, N, O and Cu atoms. The existence of no other elemental peak assures the highly purity of prepared hydrazones and copper(II) complex powders. The EDS spectrum is appeared identical for both complexes confirming the formation of the copper complexes.

HRTEM investigations

The crystallographic (T1) and amorphous (T2) structures of the copper complexes were also observed by HRTEM and the results are shown in Figs. 7 and 8. As shown in Figs. 7a and 8a and b, the copper complex T1, $[Cu(L^2)_2]$, has a crystal structure. Atomic arrangement and electron diffraction pattern expose the crystalline structure. On the other hand, as shown in Fig. 7b, the complex T2, $[Cu(H_2L^1)_2]$, has an amorphous nature. The HRTEM result supports the results of the previously mentioned XRD.

Thermal analyses

Temperature stability of the copper complexes was conceived by using thermogravimetric (TG) method carried out from 20 to 920 °C. According to TGA curves, the $[Cu(H_2L^1)_2]$ loses of ~6% of total weight in the 35–150 °C temperature range (Fig. S6). This weight loss corresponds to the remove of two moles water molecule (calcd. 5.64%) held in the lattice. This low temperature loss confirms that the water molecule does not participate in coordination. When the temperature keeps on raising, the $[Cu(H_2L^1)_2]$ complex loses ~60% of the total weight within the temperature range 150–500 °C and ~20% of the remaining weight between temperature range 500–830 °C corresponding to decomposition of the organic part of the hydrazone Schiff base ligand and finally leaving copper oxide as a residue. On the other hand, thermal degradation of $[Cu(L^2)_2]$ complex occurs in two steps (Fig. S7). In the first step, the complex loses ~55% of total weight within temperature range 230–370 °C corresponding the removal of the organic part of the acylhydrazone ligand. The last step in the 370–900 °C temperature range is the decomposition of the remaining copper(II) complexes leaving copper oxide as a residue.

Binding studies

Electronic absorption titrations

Absorption titration is an effective method to examine the binding mode of DNA with metal complexes [33–35]. Usually, when a drug interacts with DNA and forms a new complex, change in the UV–Vis absorption spectra of the drug occurs. In particularly, hypochromism with usually with a red shift due to strong stacking interactions between aromatic chromophore of molecule and the base pairs of DNA may appear in the case of an intercalative binding mode. On the other hand, the absorption intensities of drugs are increased (hyperchromism) upon increasing the concentration of CT DNA due to a damage of the CT-DNA double-helix structure. The extent of the hyperchromism is indicative of the partial or non-intercalative binding modes, such as electrostatic forces, Vander Waals interaction, hydrogen bonds and hydrophobic interaction.

The electronic absorption spectra of the copper(II) complexes in the absence and in the increasing concentrations of CT-DNA are given in the Fig. 9A and B. Upon addition of DNA, the bands at 308 nm for the $[Cu(H_2L^1)_2]$ and at 306 nm for the $[Cu(L^2)_2]$ complexes exhibit hyperchromism of 10.67% and 12.05% together

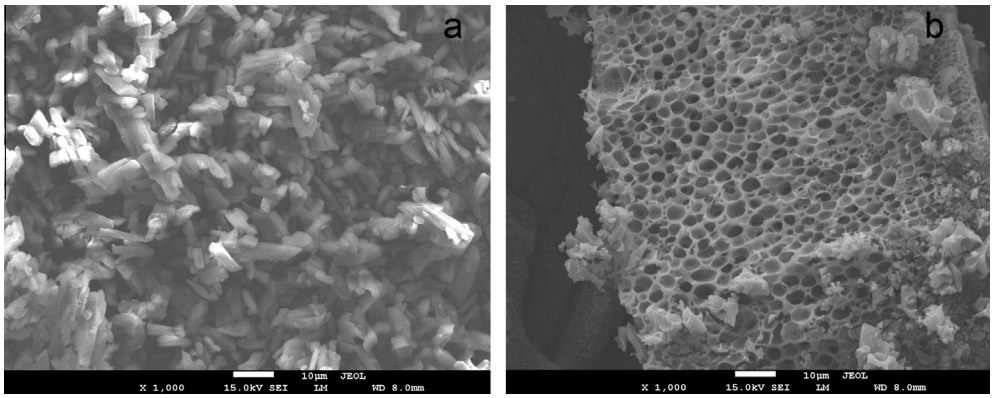

Fig. 3. The scanning electron micrographs of (a) H_3L^1; (b) $[Cu(H_2L^1)_2]$.

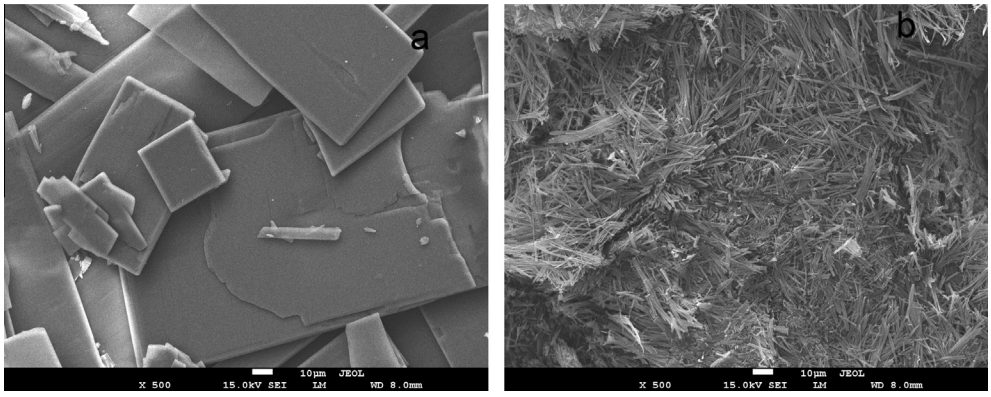

Fig. 4. The scanning electron micrographs of (a) HL^2; (b) $[Cu(L^2)_2]$.

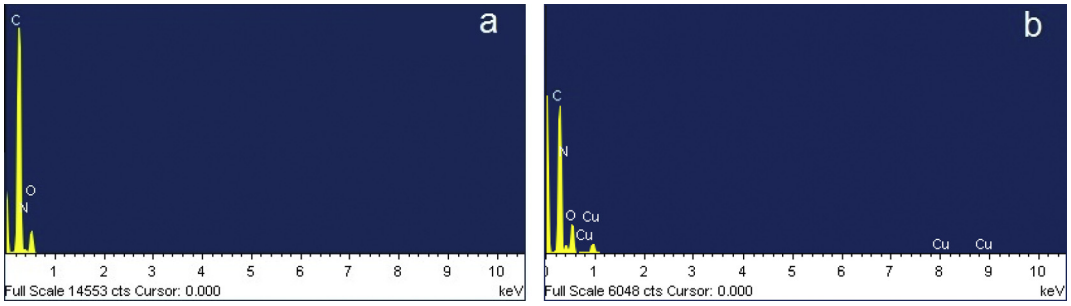

Fig. 5. Energy dispersive spectrometer of (a) H_3L^1; (b) $[Cu(H_2L^1)_2]$.

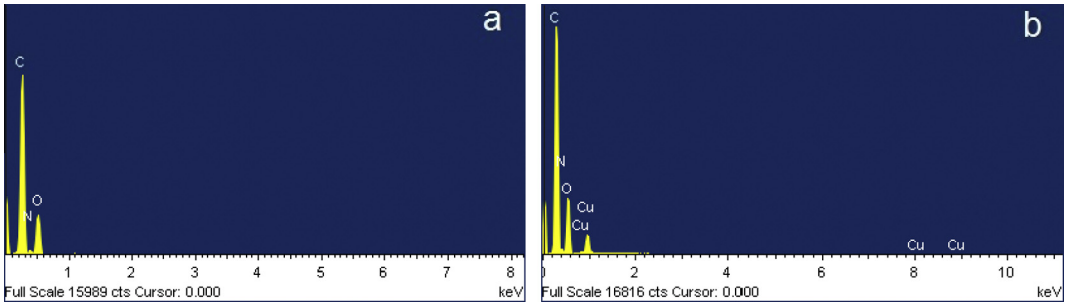

Fig. 6. Energy dispersive spectrometer of (a) HL^2; (b) $[Cu(L^2)_2]$.

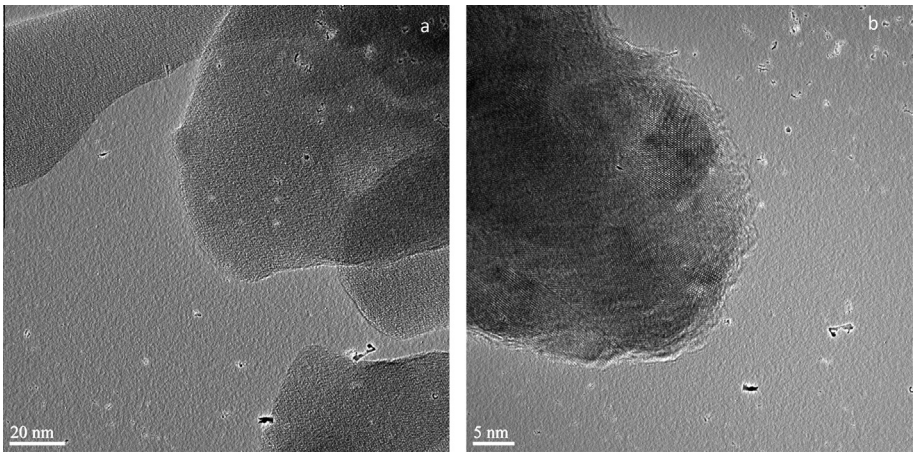

Fig. 7. HRTEM micrograph of (a) $[Cu(H_2L^1)_2]$; (b) $[Cu(L^2)_2]$.

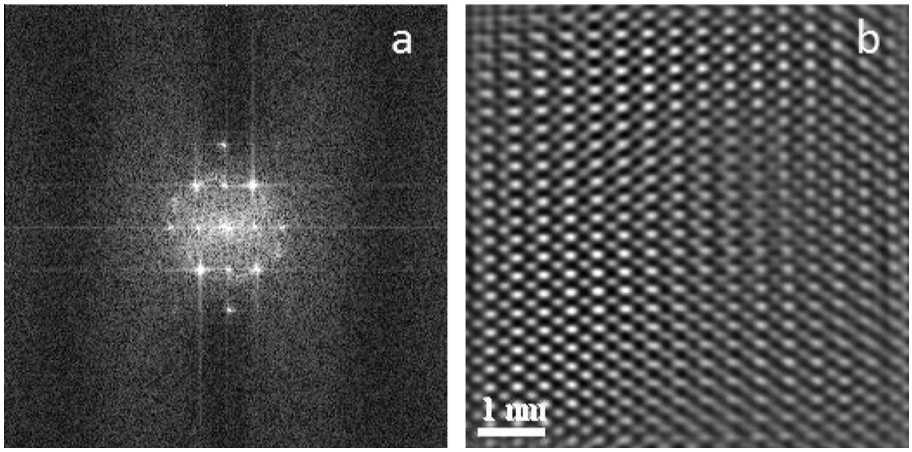

Fig. 8. (a) Diffraction pattern of $[Cu(L^2)_2]$; (b) Fast Fourier Transformation (FFT) image of $[Cu(L^2)_2]$.

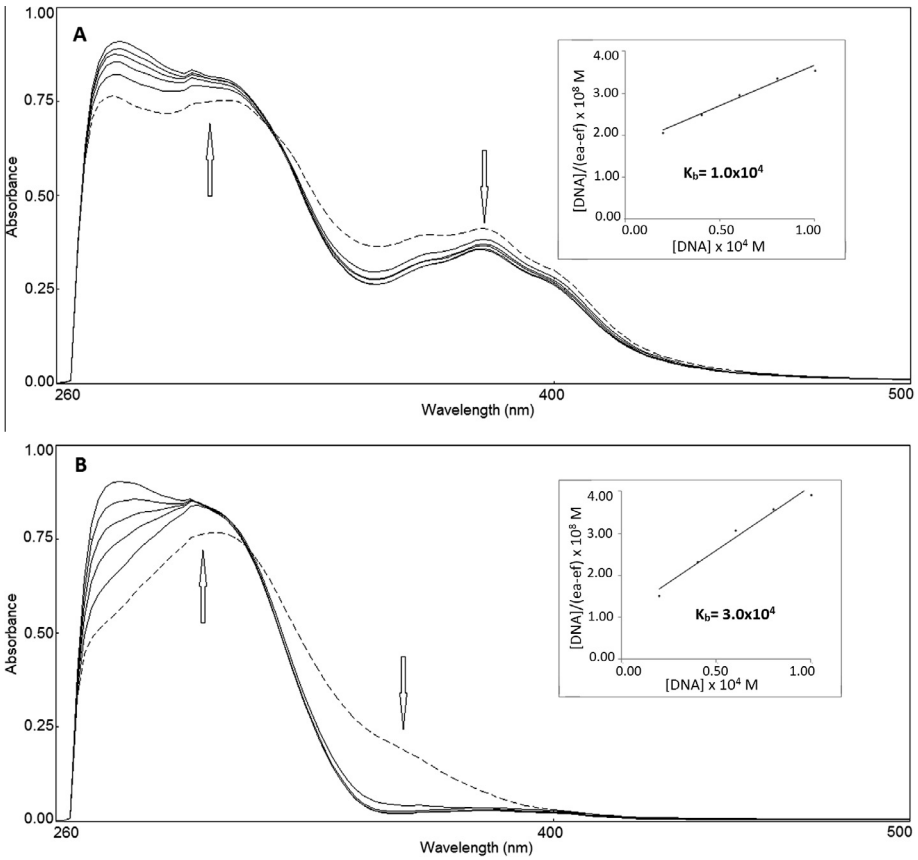

Fig. 9. Absorption spectral traces of the copper(II) complexes with increasing concentration of CT-DNA (0–100 μM). (---) absence of CT-DNA and (–––) presence of CT-DNA. (A): $[Cu(H_2L^1)_2]$, (B): $[Cu(L^2)_2]$.

with hypsochromic shifts (10 and 8 nm), respectively, indicating that both copper complexes bind and form new complexes with CT-DNA. On the other hand, the bands at 380 and 354 nm for $[Cu(H_2L^1)_2]$ and $[Cu(L^2)_2]$ complexes show only hypochromism without any shift in wavelength. A distinct isobestic point is observed at 319 and 315 nm for $[Cu(H_2L^1)_2]$ and $[Cu(L^2)_2]$, respectively, indicates the existence of the single binding mode. These changes are typical of the complexes bound to DNA through non-covalent interaction [36]. The changes in the UV–Vis spectra of the copper complexes suggest that that the binding natures of the titled copper complexes with DNA are very similar and they might bind to DNA by the groove binding or by electrostatic mode rather than by intercalative mode. The observed hypochromism could be attributed to as results of the contraction of DNA helix axes as well as the conformational changes on molecule of DNA. It can be also concluded from Fig. 9 that the electronic absorption spectra of the copper complexes are not significantly changed upon addition of DNA, suggesting that the architectures of the copper complexes are not significantly modified by binding. The binding constant, K_b, was determined by using the equation,

$[DNA]/(\varepsilon_a - \varepsilon_f) = [DNA]/(\varepsilon_o - \varepsilon_f) + 1/K_b\,(\varepsilon_o - \varepsilon_f)$, where [DNA] is the concentration of DNA in base pairs, ε_a, ε_f and ε_o correspond to A_{obsd}/[M], the extinction coefficient of the complexes and the extinction coefficient of the complex in the fully bound form, respectively, and K_b is the intrinsic binding constant. The ratio of the slope to intercept in the plot of $[DNA]/(\varepsilon_a - \varepsilon_f)$ versus [DNA] gives the value of K_b and for complex. The binding constant (K_b) values of $1.0 \times 10^4\ M^{-1}$ for $[Cu(H_2L^1)_2]$ and $3.0 \times 10^4\ M^{-1}$ for $[Cu(L^2)_2]$ suggest that $[Cu(H_2L^1)_2]$ has slight lower affinity to DNA than that of $[Cu(L^2)_2]$. However, the binding constants of these complexes are lower in comparison to those of the classical intercalators (for ethidium bromide and [Ru(phen)DPPZ]) [37,38].

Cleavage studies

The pBR322 plasmid exists in a compact supercoiled conformation (Form I). Upon formation of strand breaks, the supercoiled form of DNA is split up into the nicked circular form (Form II) and the linear from (Form III). If only one DNA strand is cleaved, the form I will relax to produce a nicked circular from. If both strands are cleaved, the form III will be produced. These three plasmid DNA conformations are distinguishable when subjected to agarose gel electrophoresis since relatively fast migration is observed for supercoiled form when the plasmid DNA is subjected to electrophoresis. The nicked circular form migrates slowly and the linear form migrates between form I and form II.

The ability of the copper complexes to cleave DNA in the presence and absence of H_2O_2 was studied by gel electrophoresis using the supercoiled form of pBR322 at 37 °C in TBE buffer [39–41]. We prepared five different concentrations of the complexes with the range from 10 to 100 μM. The titled copper(II) complexes exhibit effective cleavage activity converting the supercoiled DNA into the open circular and linear forms in the presence of hydrogen peroxide as a result of double-strand breaks over the plasmid molecule (Fig. 10). It is also clearly seen that the DNA cleavage is concentration dependence with a similar pattern for both copper complexes.

There is little difference in terms of DNA cleavage of the Cu(II) complexes between 10-50 μmol/L. With 10 and 25 μM concentrations, both copper complexes are found to cleave the supercoiled DNA to nicked and linear DNA forms and the circular supercoiled DNA band completely disappears (Fig. 10, lanes 1, 2, 12, 13). The cleavage percentage of nicked form is much higher than that of linear form for both complexes. In the case of the $[Cu(H_2L^1)_2]$, it seem that the cleavage percentages of the Form II and Form III of the plasmid DNA decreases with increasing concentration but they are still seen. (Fig. 10, lanes 3, 4, 5). On the other hand, at high concentrations (above 75 μM) of the $[Cu(L^2)_2]$ complex, the plasmid DNA is almost degraded into indistinguishable small fragments (Fig. 10, lanes 15, 16). In order to obtain information about the active chemical species effecting DNA damage, the cleavage reactions were also carried out in the presence of various ROS scavengers, that was, superoxide dismutase, NaN_3, DMSO and KI. As Fig. 11 presents, the cleavage activity of both copper complexes is reduced dramatically in the presence of SOD and KI (lines 1, 2, 5 and 6) indicating that superoxide radicals and hydrogen peroxide-derived species play a key role in the cleavage process. Moreover, NaN_3 and DMSO enhance the cleavage reaction of $[Cu(L^2)_2]$ (compare line 10 in Fig. 10 with lines 7 and 8 in Fig. 11) but inhibit that of $[Cu(H_2L^1)_2]$ (compare line 5 in Fig. 10 with lines 3 and 4 in Fig. 11). These results seem to suggest that hydroxyl radical (HO·) and singlet-oxygen ($^1O_2$) are also involved in the cleavage reaction of $[Cu(L^2)_2]$ to some extend. It may be concluded from these results that DNA cleavage promoted by the titled copper complexes in the presence of H_2O_2 takes place probably via an oxidative pathway.

In the absence of hydrogen peroxide the complexes $[Cu(H_2L^1)_2]$ and $[Cu(L^2)_2]$ exhibit less nuclease activity suggesting that

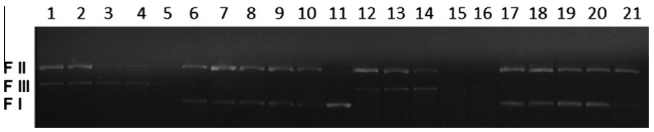

Fig. 10. Agarose gel electrophoresis of oxidative cleavage of pBR322 plasmid DNA by different concentrations of copper(II) complexes in the presence and absence of hydrogen peroxide. Lane 1: $[Cu(H_2L^1)_2]$ (10 μM) + DNA + H_2O_2, Lane 2: $[Cu(H_2L^1)_2]$ (25 μM) + DNA + H_2O_2, Lane 3: $[Cu(H_2L^1)_2]$ (50 μM) + DNA + H_2O_2, Lane 4: $[Cu(H_2L^1)_2]$ (75 μM) + DNA + H_2O_2, Lane 5: $[Cu(H_2L^1)_2]$ (100 μM) + DNA + H_2O_2, Lane 6: $[Cu(H_2L^1)_2]$ (10 μM) + DNA, Lane 7: $[Cu(H_2L^1)_2]$ (25 μM) + DNA, Lane 8: $[Cu(H_2L^1)_2]$ (50 μM) + DNA, Lane 9: $[Cu(H_2L^1)_2]$ (75 μM) + DNA, Lane 10: $[Cu(H_2L^1)_2]$ (100 μM) + DNA, Lane 11: DNA control, Lane 12: $[Cu(L^2)_2]$ (10 μM) + DNA + H_2O_2, Lane 13: $[Cu(L^2)_2]$ (25 μM) + DNA + H_2O_2, Lane 14: $[Cu(L^2)_2]$ (50 μM) + DNA + H_2O_2, Lane 15: $[Cu(L^2)_2]$ (75 μM) + DNA + H_2O_2, Lane 16: $[Cu(L^2)_2]$ (100 μM) + DNA + H_2O_2, Lane 17: $[Cu(L^2)_2]$ (10 μM) + DNA, Lane 18: $[Cu(L^2)_2]$ (25 μM) + DNA, Lane 19: $[Cu(L^2)_2]$ (50 μM) + DNA, Lane 20: $[Cu(L^2)_2]$ (75 μM) + DNA, Lane 21: $[Cu(L^2)_2]$ (100 μM) + DNA.

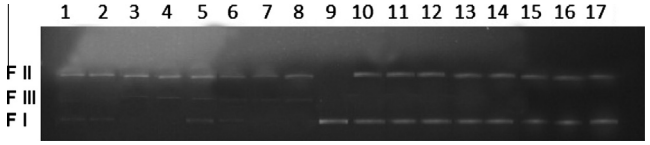

Fig. 11. Agarose gel electrophoresis of pBR322 plasmid DNA treated with the copper(II) complexes and potential inhibitors agents in the presence and absence of hydrogen peroxide. Lane 1: $[Cu(H_2L^1)_2]$ (100 μM) + DNA + H_2O_2 + SOD (100 μg/mL), Lane 2: $[Cu(H_2L^1)_2]$ (100 μM) + DNA + H_2O_2 + KI (100 μM), Lane 3: $[Cu(H_2L^1)_2]$ (100 μM) + DNA + H_2O_2 + NaN_3 (100 μM), Lane 4: $[Cu(H_2L^1)_2]$ (100 μM) + DNA + H_2O_2 + DMSO (100 μM), Lane 5: $[Cu(L^2)_2]$ (100 μM) + DNA + H_2O_2 + SOD (100 μg/mL), Lane 6: $[Cu(L^2)_2]$ (100 μM) + DNA + H_2O_2 + KI (100 μM), Lane 7: $[Cu(L^2)_2]$ (100 μM) + DNA + H_2O_2 + NaN_3 (100 μM), Lane 8: $[Cu(L^2)_2]$ (100 μM) + DNA + H_2O_2 + DMSO (100 μM), Lane 9: DNA control, Lane 10: $[Cu(H_2L^1)_2]$ (100 μM) + DNA + - SOD (100 μg/mL), Lane 11: $[Cu(H_2L^1)_2]$ (100 μM) + DNA + KI (100 μM), Lane 12: $[Cu(H_2L^1)_2]$ (100 μM) + DNA + NaN_3 (100 μM), Lane 13: $[Cu(H_2L^1)_2]$ (100 μM) + DNA + DMSO (100 μM), Lane 14: $[Cu(L^2)_2]$ (100 μM) + DNA + SOD (100 μg/mL), Lane Lane 15: $[Cu(L^2)_2]$ (100 μM) + DNA + KI (100 μM), Lane 16: $[Cu(L^2)_2]$ (100 μM) + DNA + NaN_3 (100 μM), Lane 17: $[Cu(L^2)_2]$ (100 μM) + DNA + DMSO (100 μM).

hydrogen peroxide plays an important role to aid the copper complexes in oxidative DNA cleavage reaction. Both Cu(II) complexes slightly convert the supercoiled DNA to form II, but the supercoiled form is still seen (Fig. 10), implying that they probably undergo a mainly single-strand cleavage pathway in the absence of an oxidant agent. It is also clearly seen that as the concentrations of both titled copper(II) complexes increase, the concentration of the cleaved DNA increases. It is reasonably expected in the absence of an oxidant agent the DNA cleavage is a hydrolytic. On the other hand, it is also reported that the DNA cleavage mediated by the some copper complexes occur via an oxidative mechanism without any oxidizing agent [24,39,40,42]. In this situation, the oxidative DNA cleavage can be ligand-based, possibly due to the involvement of a non-diffusible organic radical mechanism that lead to oxidative DNA cleavage. The other way is that in the presence of dioxygen, the hydrogen abstraction from the deoxyribose sugar produces dihydrogen peroxide. Then, dihydrogen peroxide couples with copper ion in a Fenton-type reaction to produce reactive diffusible oxygen species making the DNA cleavage oxidative. Considering these observations, the cleavage reactions were also performed with the radical scavengers in the absence of hydrogen peroxide. Fig. 11 shows that addition of DMSO, NaN_3, KI and SOD inhibits indeed the cleavage bye $[Cu(H_2L^1)_2]$ (compare line 16 in Fig. 10 with lines 10–13 in Fig. 11), therefore, superoxide, hydroxyl radicals and singlet oxygen species are involved in its DNA cleavage process. On the other hand, for complex $[Cu(L^2)_2]$ ROS used in this work show very little effect on the cleavage process in the absence of oxidative agent (compare line 21 in Fig. 10 with lines

14–17 in Fig. 11). These results seem to suggest that the DNA cleavage mediated by the titled complexes may also consist via an oxidative pathway. Further studies are undergoing to elucidate the cleavage mechanism.

Conclusions

In summary, two new copper(II) complexes supported by bidentate NO donor two Schiff base-hydrazone ligands derived from 4-hydroxybenzoylhydrazide and 4-hydroxyacetophenone have been synthesized and characterized using different spectroscopic techniques, including FT-IR, UV–Visible, MS, ^{1}H and 13C NMR spectroscopy, TGA, XRD, SEM and TEM. The results of electronic absorption titrations indicate that the non-covalent binding modes of these Cu(II) complexes possibly groove binding or electrostatic interaction. The complexes also exhibit efficient oxidative DNA cleavage, which significantly depends on concentrations of the complexes, in the presence of hydrogen peroxide by an oxidative mechanism involving hydrogen peroxide-derived species and superoxide radicals. Both copper(II) complexes also display slight nuclease activity in the absence of an oxidant agent. The DNA cleavage reactions carried out with the titled complexes in the absence of oxidative agent are inhibited by the presence of various radical scavengers indicating that the cleavage reaction also may undergo by an oxidative mechanism.

Acknowledgements

We thank the Scientific Research Projects Foundation of Mugla Sıtkı Koçman University for financial support of this work.

Appendix A. Supplementary material

Supplementary data associated with this article can be found, in the online version, at http://dx.doi.org/10.1016/j.saa.2014.06.133.

References

[1] K.B. Kaymakçıoğlu, E.E. Oruç, S. Unsalan, F. Kandemirli, N. Shvets, S. Rollas, D. Anatholy, Eur. J. Med. Chem. 41 (2006) 1253.
[2] P. Melnyk, V. Leroux, C. Sergheraert, P. Grellier, C. Sergheraert, Bioorg. Med. Chem. Lett. 16 (2006) 31.
[3] C. Cunha, J.M. Figueiredo, J.L.M. Tributino, A.L.P. Miranda, H.C. Castro, R.B. Zingali, C.A.M. Fraga, M.C.B. de Souza, V.F. Ferreira, E. Barreiro, J. Bioorg. Med. Chem. 11 (2003) 2051.
[4] K.K. Bedia, O. Elçin, U. Seda, K. Fatma, S. Nathaly, R. Sevim, A. Dimoglo, A. Eur. J. Med. Chem. 41 (2006) 1253.
[5] L. Savanini, L. Chiasserini, A. Gaeta, C. Pellerano, Bioorg. Med. Chem. 10 (2002) 2193.
[6] R. Albertini, S. Pinelli, P. Lunghi, Inorg. Chim. Acta 286 (1999) 134.
[7] H. Elo, I. Sunila, P. Lumme, Inorg. Chim. Acta 136 (1987) 61.
[8] T. Todorovic, U. Rychlewska, B. Warzajtis, D. Radanovic, N. Filipovic, I. Pajic, D. Sladic, K. Anđelkovic, Polyhedron 28 (2009) 2397.
[9] B.D. Wang, Z.Y. Yang, Q. Wang, T.K. Cai, P. Crewdson, Bioorg. Med. Chem. 14 (2006) 1880.
[10] Y.Y. Karabach, A.M. Kirillov, M. Haukka, M.N. Kopylovich, A.J.L. Pombeiro, J. Inorg. Biochem. 102 (2008) 1190.
[11] U. Schuchardt, W.A. Carvalho, E.V. Spinace, Synlett 10 (1993) 713.
[12] M.F. Iskander, S.E. Zayan, M.A. Khalifa, L. El-Sayed, J. Inorg. Nucl. Chem. 36 (1974) 551.
[13] J.D. Ranford, J.J. Vittal, Y.M. Wang, Inorg. Chem. 37 (1998) 1226.
[14] K.E. Erkkila, D.T. Odom, J.K. Barton, Chem. Rev. 99 (1999) 2777.
[15] B. Lippert, Coord. Chem. Rev. 200 (2000) 487.
[16] J.K. Barton, E. Lolis, J. Am. Chem. Soc. 107 (1985) 708.
[17] D. Charles, J.H. Turner, C. Redmond, Int. J. Obstet. Gynecol. 80 (2005) 264.
[18] S. Apelgot, J. Coppey, A. Fromentin, E. Guille, M.F. Poupon, A. Roussel, Anticancer Res. 6 (1986) 159.
[19] J.R.J. Sorenson, In Metal Ions in Biological Systems, in: H. Sigel, M. Dekker (Eds.), Newyork, 14 (1982) 77.
[20] R.K. Gouch, T.W. Kensler, L.W. Oberley, R.J. Sorenson, in: K.D. Karlin, J. Zubieta (Eds.), Biochem. Inorg. Copper Chem 1 (1986) 139.
[21] A.P. Rajput, S.S. Rajput, Int. J. Pharm. Pharm. Sci. 3 (Suppl 4) (2011) 346.
[22] J. Marmur, J. Mol. Biol. 3 (1961) 208–218.
[23] C.V. Kumar, E.H. Asuncion, J. Am. Chem. Soc. 115 (1993) 8547–8553.
[24] C. Gokce, R. Gup, J. Photochem. Photobiol. B Biol. 122 (2013) 15.
[25] C. Gokce, R. Gup, Appl. Organometall. Chem. 27 (2013) 263.
[26] R. Gup, B. Kırkan, Spectrochim. Acta A 64 (2006) 809.
[27] R. Gup, B. Kırkan, Spectrochim. Acta A 62 (2005) 1188.
[28] M.J. Li, T.Y. Lan, Z.S. Lin, C. Yi, G.N. Chen, J. Biol. Inorg. Chem. 18 (2013) 993.
[29] A.A.R. Despaigne, J.G. Da Silva, A.C.M. Do Carmo, O.E. Piro, E.E. Castellano, H. Beraldo, J. Mol. Struct. 920 (2009) 97.
[30] A.P. Rebolledo, G.M. Lima, L.N. Gambi, N.I. Speziali, D.F. Maia, C.B. Pinheiro, J.D. Ardisson, M.E. Cortes, H. Beraldo, Appl. Organometall. Chem. 17 (2003) 945.
[31] A.A.R. Despaigne, J.G. Da Silva, A.C.M. Do Carmo, F. Sives, O.E. Piro, E.E. Castellano, H. Beraldo, Polyhedron 28 (2009) 3797.
[32] L.L. Koh, O.L. Kon, K.W. Long, J.D. Ranford, A.L.C. Tan, Y.Y. Tjan, J. Inorg. Biochem. 72 (1998) 155.
[33] J.K. Barton, A.T. Danishhefsky, J.M. Goldberg, J. Am. Chem. Soc. 106 (1984) 2172.
[34] A.M. Pyle, J.P. Rehmann, J.P. Meshoyrer, C.V. Kumar, N.J. Turro, J.K. Barton, J. Am. Chem. Soc. 111 (1989) 3051.
[35] T. Hirohama, Y. Kuranuki, E. Ebina, T. Sugizaki, H. Arii, M. Chikira, P.T. Selvi, M. Palaniandavar, J. Inorg. Biochem. 99 (2005) 1205.
[36] M. Cory, D.D. McKee, J. Kagan, D.W. Henry, J.A. Miller, J. Am. Chem. Soc. 107 (1985) 2528.
[37] K.H. Reddy, P.S. Reddy, P.R. Babu, J. Inorg. Biochem. 77 (1999) 169.
[38] K. Dhara, J. Ratha, M. Manassero, X. Wang, S. Gao, P. Banerjee, J. Inorg. Biochem. 101 (2007) 95.
[39] P.U. Maheswari, S. Barends, S. Özalp-Yaman, P. Hoog, H. Casellas, A. Teat, C. Massera, M. Lutz, A.L. Spek, G.P. Wezel, P. Gamez, J. Reedijk, Chem. Eur. J. 13 (2007) 5213.
[40] S.S. Massoud, F.R. Louka, W. Xu, R.S. Perkins, R. Vicente, J.H. Albering, F.A. Mautner, Eur. J. Inorg. Chem. 23 (2011) 3469.
[41] N.J. Garrido, L. Perello, R. Ortiz, J. Inorg. Biochem. 99 (2005) 677.
[42] P.P. Silva, W. Guerra, J.N. Silveira, A.M.C. Ferreira, T. Bortolotto, F.L. Fischer, H. Terenzi, A. Neves, E.C. Pereira-Maia, Inorg. Chem. 50 (2011) 6414.